S_BRICK: A CONSTITUTIVE MODEL FOR SOILS AND SOFT ROCKS

S_BRICK: KONSTITUTIVNI MODEL ZA ZEMLJINE IN MEHKE KAMNINE

Vladimir Vukadin
Institute for Mining, Geotechnology and Environment (IRGO)
Slovenčeva 93, 1000 Ljubljana, Slovenia

Vojkan Jovičić *(corresponding author)*
Institute for Mining, Geotechnology and Environment (IRGO)
Slovenčeva 93, 1000 Ljubljana, Slovenia
E-mail: vojkan.jovicic@irgo.si

Keywords

structure, constitutive material models, soft rocks and hard soils, numerical modelling, destructuring

Ključne besede

struktura, konstitutivni materialni modeli, mehke kamnine in trde zemljine, numerično modeliranje, destrukturizacija

Abstract

Materials known in the literature as hard soils and soft rocks are widely spread, natural materials that are commonly encountered in engineering practise. It was demonstrated that some of these materials can be described through the general theoretical framework for structured soils set by Cotecchia and Chandler [14], which takes into account the structure as an intrinsic property present in all natural geological materials. Based on laboratory results and existing theoretical frameworks, the development of a constitutive model for structured materials was carried out. The model formulated in strain space named BRICK [27, 29] was chosen as the base model and was further developed by adding features to model both the structure and the processes of destructuring. The new model was named S_BRICK and was first presented on a conceptual level, in which the typical results of modelling structured and structureless (reconstituted) materials on different stress paths were compared within the solutions of the Cotecchia and Chandler [14] theoretical framework. The S_BRICK model was validated on three materials, i.e., Pappadai clay, North-Sea clay and Corinth marl, thus covering a wide range of natural, structured materials. The results showed that S_BRICK was able to successfully model the stress-strain behaviour typical for hard-soil and soft-rock materials, in general.

Izvleček

Materiali, ki so poznani v literaturi kot trde zemljine ali mehke kamnine, so široko razširjeni naravni materiali pogosto prisotni v inženirski praksi. Pokazano je, da se določeni tovrstni materiali lahko opišejo s pomočjo teorijskega okvirja za strukturirana tla, ki so ga razvili Cotecchia in Chandler [14], in sicer na ta način, da so upoštevali notranjo strukturo, ki je prisotna v vseh naravnih geoloških materialih. Razvoj konstitutivnega modela za strukturirane zemljine je bil narejen na podlagi rezultatov laboratorijskih raziskav in z uporabo obstoječih teorijskih okvirjev. Konstitutivni model BRICK [27, 29], ki je bil razvit v prostoru relativnih deformacij, je bil izbran za osnovni model in je nadgrajen z dodatnimi lastnostmi, da bi bil lahko uporaben za modeliranje strukture in tudi procesa destrukturizacije. Novi model, imenovan S_BRICK, je najprej predstavljen na konceptualnem nivoju, v katerem so tipični rezultati modeliranja strukturiranih in ne-strukturiranih (rekonstituiranih) materialov primerjani z rešitvami iz Cotecchia in Chandler-ovega [14] teorijskega okvirja. Model S_BRICK je validiran na tri materiale: pappadaiska glina, glina iz severnega morja in korintski lapor. Na ta način je validacija modela zajela široki razpon naravnih materialov. Rezultati so pokazali, da model S_BRICK lahko uspešno modelira napetostno-deformacijsko obnašanje, ki je tipično za trde zemljine ali mehke kamnine.

1   INTRODUCTION

The BRICK model, developed by Simpson [27, 29] for overconsolidated clays, was chosen to be the base model for the development of the constitutive model called S_BRICK, aiming to model structured materials such as hard soils and soft rocks. This was mainly due to the BRICK model's ability to model the non-linear, stress-strain response of soil and the recent stress--history effect [5], which are both the main features of the mechanical behaviour characterised by kinematic hardening.

In the first part of the paper the framework for structured soils developed by Cotecchia and Chandler [14] is presented together with a brief description of the original BRICK model. This is followed by an explanation of the S_BRICK model formulation, in which the additional features are given to account for the influence of the structure on the mechanical behaviour of natural materials. A particular feature of the S_BRICK model is its ability to model destructurisation. It was soon understood that the modelling of structured natural materials could not be successful without taking into account the processes of structure decay following the plastic deformation. The methodology of modelling destructuring in S_BRICK is explained and the parameter determination procedure is given on a conceptual level.

Finally, the validation of the S_BRICK model was carried out on three natural materials: Pappadai clay, North-Sea clay and Corinth marl. While the Pappadai clay and the North-Sea clay are heavily overconsolidated clays and can be classified as hard soils, Corinth marl is a typical representative of soft rock, with a complex geological history and the resulting mechanical properties. Those three materials were chosen to demonstrate the ability of S_BRICK to cover the main features of the mechanical behaviour of a wide range of natural, structured materials.

2   THEORETICAL BACKGROUND

2.1   Structured materials

Kavvadas [21] and Kavvadas and Anagnostopoulos [22] suggested that the principles of soil mechanics could be applied to the modelling of hard soils and soft rocks as long as the behaviour of the natural material is not influenced significantly by large-scale discontinuities. It is widely accepted that, apart from including the important features of the mechanical behaviour of soils, such as nonlinearity, small strain stiffness and the influence

of volumetric and kinematic hardening, a constitutive model has to include the effects of structure and destructuring in order to describe the behaviour of natural geological materials [25, 10, 14, 23, 26, 7, 16, 2, 17, 11].

The origins of the structure in natural soils are complex and can be attributed to different processes and different physical and chemical conditions during and after sedimentation. Hence, there are many different classifications and definitions that take into account the different aspects of structure. Lambe and Whitman [24] stated that structure is a combination of the fabric and the bonding in which the fabric represents the arrangement of the soil particles and the bonding represents the chemical, physical or any other types of bonds between the particles. Bonding has predominant effects in rocks, while in soils the influence of fabric is more important. It is obvious that according to this definition, structure is present in both natural and reconstituted geological materials, because no matter how much material is remoulded or destructured, it still has some type of fabric. Nevertheless, from the mechanical point of view, the influence of structure in reconstituted materials is the benchmark reference state representing the lower bound for the strength and the stiffness of natural materials.

An example of the influence of structure on state boundary surfaces (SBSs) for undisturbed, partly destructured and reconstituted Pappadai clay is shown in Figure 1 (after Cotecchia and Chandler [14]). It can be seen in the q/p' diagram (p' is mean effective stress and q is the deviator stress) normalized with the mean effective stress $p'_e{}^*$ (taken at an isotropic reconstituted normal compression line at the same specific volume as for the intact clay) that the influence of structure is manifested by the size of the SBSs, resulting in the higher strength and stiffness of the undisturbed material in comparison with the partly destructured or reconstituted Pappadai clay. Cotecchia and Chandler [14] and Kavaddas and Anagnostopoulos [22] and the other authors differ on the classification and the mechanisms of the structure development, but they all nevertheless agree that the position of the in-situ state in volumetric space, i.e., the distance of the yield stress from the intrinsic compression line, controls the compression and the strength behaviour of natural soils. The intrinsic compression line here refers to the properties of reconstituted materials, representing the lower bound for the normal compression lines of natural materials.

The key element of the structure is stability, as Baudet [6] and Baudet and Stallebrass [7] emphasise, so that the stable structure is predominantly governed by the fabric, while the unstable structure is predominantly
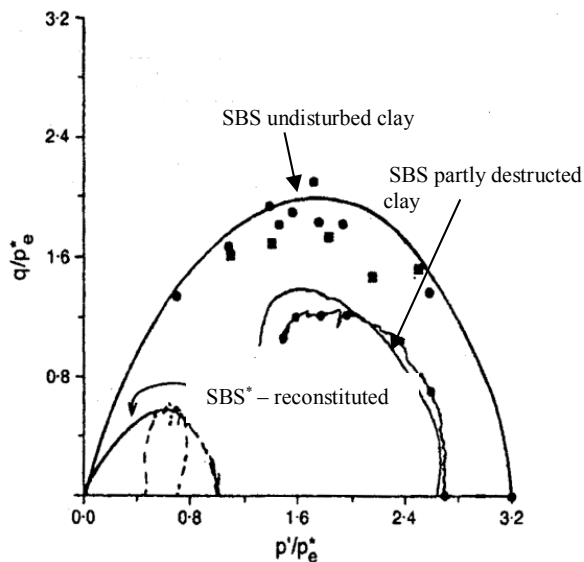
Figure 1. Influence of the structure on the SBS of undisturbed, partly destructed and reconstituted Pappadai clay (after Cotecchia & Chandler, [14]).

governed by the bonding. Destructuring is caused by the plastic straining and is responsible for the decreasing of the SBS, as shown in Figure 1, and thus a reduction in the strength and the stiffness of the natural soil. The materials that show a certain degree of destructuring are classified as meta-stable, in which both elements of the structure (fabric and bonding) are still present. According to Leroueil and Vaugan [25], yielding and hence the plastic straining, causing destructuring can result by

following shearing, compression and swelling stress paths inside the SBS. However, these mechanisms of destructuring are still not fully understood, which was and would be an obvious obstacle to the development of the models that simulate the behaviour of natural materials.

2.2 Theoretical frameworks

The proposed S_BRICK model was developed using the theoretical concepts of elasto-plasticity and critical state soil mechanics [30, 4] in a wider sense and the approach of Simpson [27] in developing the basic BRICK model. A further step in the model's development was made by using the theoretical framework for structured soils developed by Cotecchia and Chandler [14]. In this framework the influence of the structure (S) is quantified by the difference in the sizes of the SBSs of the structured and reconstituted materials, which are similar in shape. The framework is conceptually presented in Figure 2 in the q-p'-v space (v represents the specific volume), showing the two idealised boundary surfaces for reconstituted and structured materials. Cotecchia and Chandler [14] postulated that the parameter of shear sensitivity St, which is the ratio between the peak shear strengths of the natural or structured (q_{peak}) and the reconstituted material (q^*_{peak}), is equal to the parameter of stress sensitivity S_σ which is defined as the ratio of the effective stresses for natural and reconstituted soils, taken at the same specific volume for isotropic (p'_{ei}/p'^*_{ei}) or normal compression lines (p'_{eK0}/p'^*_{eK0}).
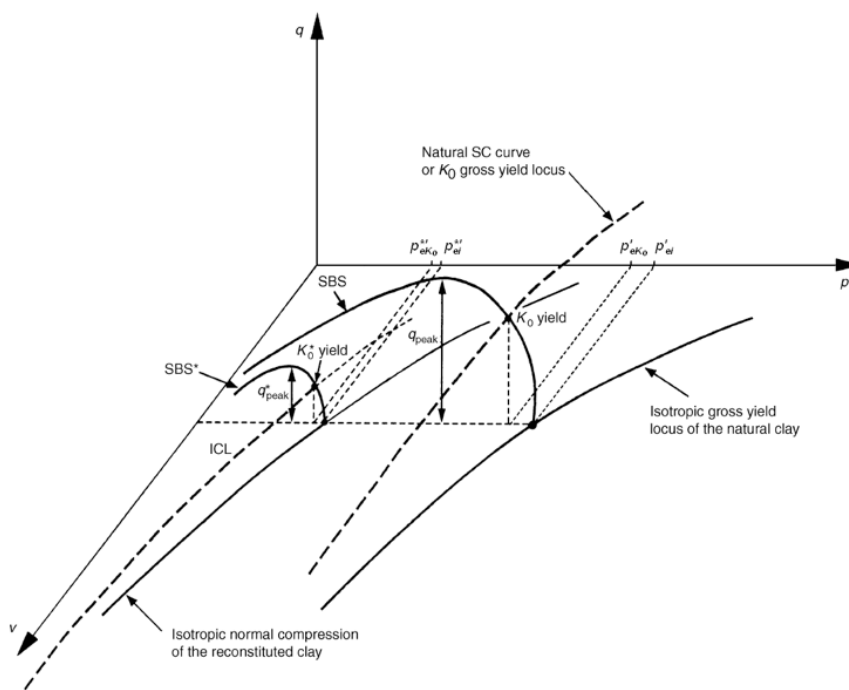

Figure 2. Theoretical framework for structured and reconstituted material in the q-p'-v space (after Cotecchia & Chandler, [14]).

The relationship is given by the following expression:

$$S = S_t = q_{peak} / q^*_{peak} = S_\sigma = p'_{ei} / p'^*_{ei} = p'_{eKo} / p'^*_{eKo} \qquad (1)$$

The value of the parameter S for the reconstituted material is equal to 1; therefore, the SBSs of the reconstituted and structured materials should coincide when plotted together in the normalized space $q/(Sp'_e{}^*)$-$p'/(Sp'_e{}^*)$, which takes into account the structure (S) and the volume ($p'_e{}^*$). The framework was validated by Cotecchia and Chandler [14] for Sibari, Bothkennar and Pappadai clays. The theoretical framework was also subsequently validated by Baudet [6] and Baudet and Stallebrass [7] for different materials, ranging from soft to hard clays. Even though the data on soft rocks in the literature are not as extensive as those on soft and hard clays, there is enough evidence to suggest that the basic concepts of this theoretical framework can also be applied to soft rocks [18, 23, 1].

2.3 Basic concepts of the BRICK model

The constitutive model for the structured soils S_BRICK originates from the BRICK model developed by Simpson [27, 29]. The BRICK model was developed to model the behaviour of over-consolidated clays, but was also successfully used to model soft or normally consolidated soils. The model includes many important features of the soil behaviour, including isotropic and kinematic hardening, and can model the stress-strain nonlinearity and the recent stress-history effect [5]. The means of formulation for the BRICK model are such that it is not obvious how the BRICK model is related to the theoretical concept of critical state soil mechanics or how the model can be extended within the theoretical framework for structured soils developed by Cotecchia and Chandler [14]. An attempt is made to underline those features of the BRICK model so that the further development to the S_BRICK model can be understood. The background and the formulation of the BRICK model are given in detail by Simpson [27, 29] and a more updated version, which includes a 3D formulation, is given by Ellison et al. [15].

The BRICK model is formulated in the strain space defined by the six strain invariants ε_i (i=1–6) in which the first one represents the volumetric component and other five represent the deviatoric components of the strain. The main idea is explained by the analogy of bricks and strings shown in Figure 3a, in which a man (representing the current strain state) is pulling a certain, but definitive, number of bricks that are attached to him by strings of different lengths (representing the current strain path, causing a plastic deformation of different
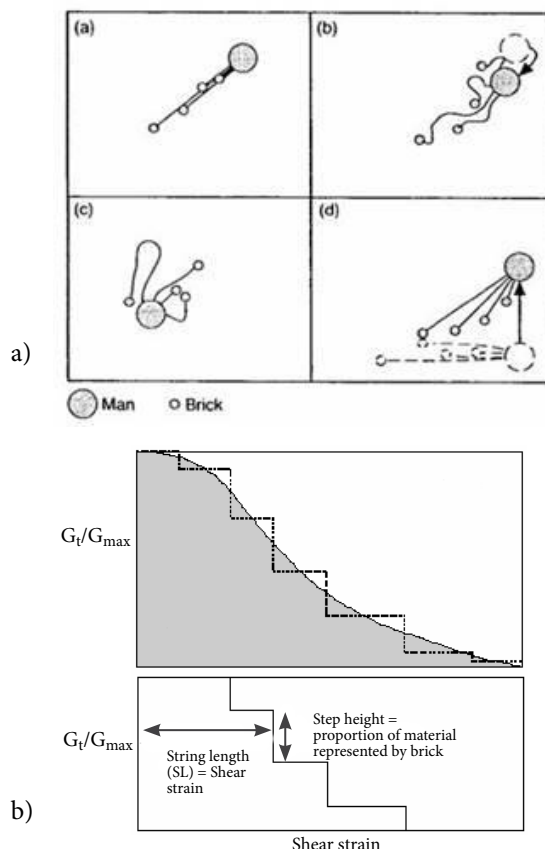

a)

b)

Figure 3. The concept of the BRICK model:
a) brick and string analogy and b) discretization of the S-shaped curve (after Simpson, [27]).

magnitude). The analogy is essentially a way to discretise the decay of the tangent shear stiffness with the shear strain shown in Figure 3b in the shape of the normalised *S-shaped* curve. The strings (*SL* – string length) are given in a stepwise fashion, in which the height of each step indicates the proportion of the material being represented by a single brick. At very small strains the material is completely elastic, all the strings are slack and the bricks do not move. As the straining proceeds, the first brick starts to move, the plastic strain begins and there is a drop in the stiffness of the material. With continuous straining, more and more bricks are being pulled, there is more plasticity and there is a further drop in the stiffness until the material is fully plastic and the stiffness limits towards zero. When the stress path is changed initially, all the strings are slack, so that the immediate response is elastic. It should be noted though, that many stress paths starting from an in-situ state will not be fully elastic at small strains because some strings will remain taut. The plastic strain develops in the direction of the string orientation so that fully plastic behaviour does not occur until all the strings are all taut and aligned in the direction of the strain increment.

With the BRICK analogy, the concepts of non-linearity, recent stress history and kinematic hardening are all being accounted for. Simpson [27] also demonstrated that the area beneath the normalized *S-shaped* curve is equal to sinϕ', and thus determines the maximum angle of shearing resistance for the effective stresses ϕ' defining the strength response of the model. Simpson [28] also showed how the model could be viewed as a set of nested yield surfaces, expressed in the strain space.

The stiffness response of the BRICK model in the elastic range is accounted for by the parameter ι that represents the correlation of the elastic volumetric modulus with the mean effective stress. The *S-shaped* curve and the elastic parameter ι are additionally modified by a volumetric state parameter that accounts for the changes to the stiffness and the strength. Therefore, as for the other kinematic hardening models, the correct modelling of a stress history is of crucial importance for the correct model predictions. The state parameter ψ_B, an important feature of the BRICK model, is used to the same effect of accounting for isotropic hardening as is the overconsolidation ratio used in the theory of critical state soil mechanics. As will be explained later, the concept of state, which was defined in a similar way as proposed by Been and Jeffries [8], was used as a means to extend the BRICK model within the theoretical framework developed by Cotecchia and Chandler [14] for structured soils. The state parameter ψ_B in the BRICK model is given by the following expression:

$$\psi_B = \varepsilon_\upsilon - \varepsilon_{\upsilon 0} - \lambda \ln\left(p'/p'_0\right) \qquad (2)$$

In this expression, ψ_B represents the distance of the current volumetric-stress state given by p' (mean effective stress) and ε_υ (volumetric strain) from the reference state represented by the normal compression line defined by p'_0, λ and $\varepsilon_{\upsilon 0}$ in the ε_υ-lnp' plane, as shown in Figure 4. As it is assumed that the reconstituted material has not undergone any straining, $\varepsilon_{\upsilon 0}$ is set to zero and p'_0 is taken at the arbitrary (non-zero but small) value of 2 kPa. Simpson [27] introduced the influence of the state on stiffness and the strength using the parameter β, which he subsequently divided into two parameters, β_G and β_φ, so that the influence of the state on the stiffness and strength, respectively, is given by the following two expressions:

$$SL = SL_{current} \frac{\left(1 + \beta_\varphi \psi_B\right)}{\left(1 + \beta_G \psi_B\right)} \qquad (3)$$

$$\iota = \iota_{current}\left(1 + \beta_G \psi_B\right) \qquad (4)$$

It is clear from Equation 3 that the string lengths (*SLs*) are influenced by both the parameters β_G and β_φ, which means that the influence on the stiffness and the strength is not fully decoupled. In total, the BRICK model requires eight parameters, from which five can be determined using conventional laboratory testing (λ, κ, ι, ν and the shape of S curve), one that can be used as a constant (μ-Drucker-Prager parameter defining the shape of a State Boundary Surface in Π-plane) and the two (β_G and β_φ) can be determined by back-analysing conventional laboratory tests through a trial-and-error process. It will be shown later that the values of most of the parameters fall into relatively narrow intervals, so the values given by Simpson [27, 29] for London clay, given in Table 1, could be used as suitable starting values for any other clay. Furthermore, the *S-shaped* curve, which is given in normalized form, seems to be similar for all hard-soils and soft-rock materials, which were the subject of this research, as will be demonstrated latter.
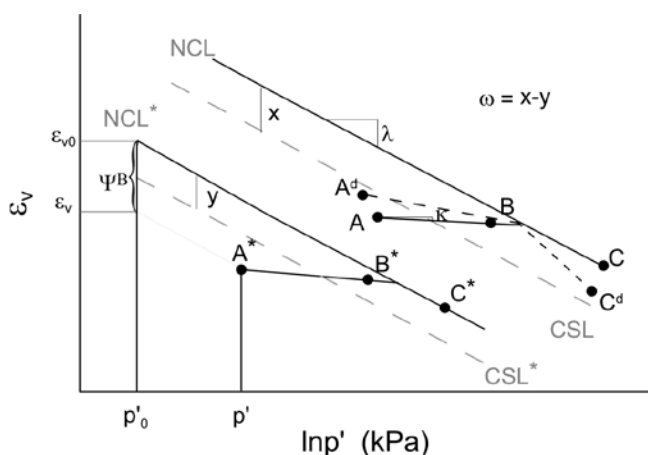

Figure 4. Concept of the state parameter Ψ_B as modeled in BRICK, definition of the parameter ω, and locations of the necessary triaxial tests for the parameter determination for S_BRICK.

3   FORMULATION OF THE S_BRICK MODEL

The newly developed model was named S_BRICK to indicate the ability to model structured soils, while the original name was preserved, indicating that all the features of the BRICK model were preserved. A single-element program was developed as a tool for numerical simulations of soil behaviour using the S_BRICK model in 3D strain space.

3.1   Modelling of a structure

The influence of structure is accounted for by the introduction of the two new parameters α and ω. The first parameter α is used to proportionally increase or decrease the size of the string lengths (*SLs*) and thus of the area beneath the *S-shaped* curve. This has a direct

Table 1. S_BRICK parameters for natural and reconstituted London clay, Pappadai clay, North-Sea clay and Corinth marl.

Parameter	London clay	Pappadai natural	Pappadai reconstituted	North-Sea natural		North-Sea reconstituted	Corinth natural
				Cape shore	Ferder		
Basic BRICK parameters							
Λ	0.1	0.254	0.204	0.1	0.1	0.1	0.6
K	0.02	0.029	0.046	0.02	0.02	0.02	0.005
I	0.0041	0.0048	0.0048	0.0041	0.0041	0.0041	0.0041
β_G	4	4	4	4	4	4	4
β_φ	3	3	3	3	3	3	3
N	0.2	0.2	0.2	0.2	0.2	0.2	0.2
M	1.3	1.3	1.3	1.3	1.3	1.3	1.3

S-curve (as defined in BRICK and in S_BRICK for $\alpha=0.8$)

String Length

0.000083	0.00021	0.00041	0.00083	0.0022	0.0041	0.0082	0.021	0.041	0.08

G_{tan}/G_{max}

0.92	0.75	0.53	0.29	0.13	0.075	0.044	0.017	0.0035	0.0

Parameter	London clay	Pappadai natural	Pappadai reconstituted	North-Sea natural		North-Sea reconstituted	Corinth natural
				Cape shore	Ferder		
S_BRICK parameters defining structure and destructurisation							
α/α_k		0.7/0.6	0.6/0.6	0.85/0.85	0.85/0.85	0.85/0.85	1.1/1.1
$\varphi(°)$	21	21	18	25.5	25.5	25.5	33
ω/ω_k	-	0.12/0	0/0	1.8/0	1.2/0	0.06/0	1.0/0
x^c_1/x^c_2	-	20 / 80	0/0	0/200	0/500	0/0	0/3000
y^c_1/y^c_2	-	0/0	0/0	0/0	0/0	0/0	0/1000
x^{sh}_1/x^{sh}_2	-	0/0	0/0	0/900	0/300	0/0	0/3000
y^{sh}_1/y^{sh}_2	-	0/0	0/0	0/1000	0/450	0/0	0/3000
x^{sw}_1/x^{sw}_2	-	0/0	0/0	0/200	0/500	0/0	0/0
y^{sw}_1/y^{sw}_2	-	0/0	0/0	0/0	0/0	0/0	0/0

influence on the value of the maximum angle of the shearing resistance and hence the strength response of the model. As indicated earlier, the normalized *S-shaped* curve for London clay was taken as a reference shape. The parameter α is implemented by modifying the string lengths using the following expression:

$$SL = SL_{current} \frac{(1+\beta_\varphi \psi_B)}{(1+\beta_G \psi_B)} \alpha \qquad (5)$$

The lower and upper range for the parameter is defined so that the maximum angle of the shearing resistance φ ranges from 18º ($\alpha=0.6$) to 36º ($\alpha=1.2$), which is considered as a reasonable range of φ for natural materials, which can be easily extended at both ends. With a value $\alpha=0.7$, S_BRICK uses the same *S-shaped* curve as the basic BRICK model defined by Simpson [27]. The influence of the parameter α is graphically presented in Figure 5 for $\psi_B = 0$, together with its proposed range of values.
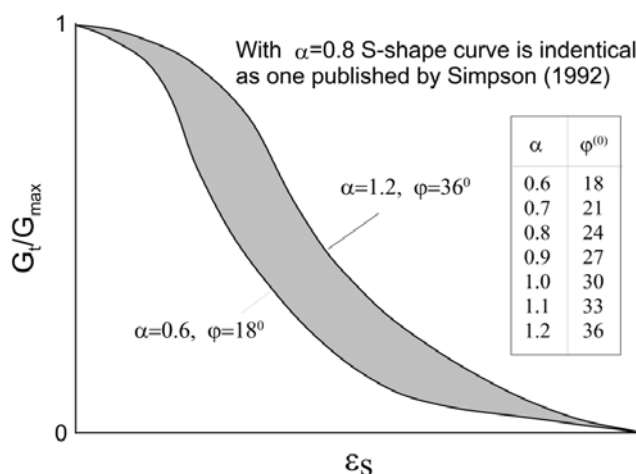
Figure 5. Influence of the parameter α on *S-shaped* curve and its characteristic values.

The second parameter ω modifies the ψ_B parameter to account for the influence of structure. The definition of ω is graphically presented in Figure 4. It is best understood as an increase of the distance, in terms of volumetric strain, between the normal compression line and the critical state line of the structured material in comparison with that of the reconstituted material. In a numerical sense, the effect of parameter ω is to increase the apparent overconsolidation of the soil. It is used to modify Equation 2 with the following expression:

$$\psi_B = \varepsilon_\upsilon - \varepsilon_{\upsilon 0} - \lambda \ln\left(p' / p_0'\right) + \omega \qquad (6)$$

It is evident from Equations 3 and 4 that the state parameter influences both the ι parameter (elastic stiffness) and the string lengths (*SLs*) of the normalized *S-shaped* curve (strength) so there would be inevitably some overlapping of the influences of the parameters α and ω on the model behaviour. However, the influence of the parameter ω on ι and hence the stiffness is larger than the influence on the *S-shaped* curve and hence the strength because the *S-shaped* curve is modified by the ratio of the state parameters (Equation 3). The parameter ω is therefore the key parameter for modelling the stiffness increase and the parameter α is the key parameter for modelling the strength increase caused by the presence of structure.

3.2 Modelling of destructuring

Destructuring is modelled using the both parameters α and ω. They are given in the form of normalised exponential functions of strains to account for the presumed logarithmic nature of the destructuring [18, 23]. The rates of destructuring are made dependent on the sum of the volumetric and shear components of the plastic strains, as shown in the following two expressions:

$$\alpha_t^{c,sh,sw} = \alpha_k + \left(\alpha - \alpha_k\right)\exp\Big[-\Big(x_1^{c,sh,sw}\left(\varepsilon_\upsilon^{pl} + \delta\varepsilon_\upsilon^{pl}\right) +$$
$$y_1^{c,sh,sw}\left(\varepsilon_s^{pl} + \delta\varepsilon_s^{pl}\right)\Big)\Big] \qquad (7)$$

$$\omega_t^{c,sh,sw} = \omega_k + \left(\omega - \omega_k\right)\exp\Big[-\Big(x_2^{c,sh,sw}\left(\varepsilon_\upsilon^{pl} + \delta\varepsilon_\upsilon^{pl}\right) +$$
$$y_2^{c,sh,sw}\left(\varepsilon_s^{pl} + \delta\varepsilon_s^{pl}\right)\Big)\Big] \qquad (8)$$

in which the symbols represent the following:

α, ω	initial values of parameters for natural materials
α_k, ω_k	final values of parameters for natural materials that were destructed
$\alpha_k{}^*$, $\omega_k{}^*$	values of structure parameters for reconstituted materials
$\alpha_i^{c,sh,sw}$, $\omega_i^{c,sh,sw}$	current values of structure parameters in compression (c), shear (sh) or swelling (sw)
ε_v^{pl}, ε_s^{pl}	volumetric and shear component of plastic strain
$\delta\varepsilon_v^{pl}$, $\delta\varepsilon_s^{pl}$	increment of volumetric and shear component of plastic strain
$x_1^{c,sh,sw}$, $y_1^{c,sh,sw}$	parameters that quantify influence of volumetric and deviatoric plastic strain on destructuring of parameter α
$x_2^{c,sh,sw}$, $y_2^{c,sh,sw}$	parameters that quantify influence of volumetric and deviatoric plastic strain on destructuring of parameter ω

Parameters α^*_k and ω^*_k are not implicitly shown in Equations 7 and 8. They are used in the model to represent the structure in reconstituted materials and also implicitly for the materials with unstable structures, for which α_k and ω_k in the destructuring are approaching, or are equal to α^*_k and ω^*_k. Destructuring in S_BRICK is implemented separately by introducing different parameters x_1, x_2 and y_1, y_2, for shearing, compression and swelling. The decoupling of the destructurisation on the volumetric and shear components of strain at different stress paths gives an additional flexibility to the model. It is also assumed that the destructuring in the shearing is governed by both volumetric and deviator components of the plastic strain.

3.3 Parameter determination for structure and destructuring

For a complete parameter determination three drained and three undrained triaxial shearing tests and one triaxial compression test should be carried out on both the natural and the reconstituted material, which makes fourteen triaxial tests in total. As will be shown later, this number can be significantly reduced by the robustness of the model. The triaxial compression tests should be carried out to sufficiently high stresses so that destructuring of the natural material in compression can be determined. Triaxial tests should include measurements of the stiffness at very small strains and should be carried out at the different initial states shown in Figure 4, so that the material response is obtained for the overconsolidated (A, A*), normally consolidated (B, C, B*, C*) and destructured states (A^d, C^d). The asterisk sign * is used here to denote the states of the reconstituted material, while the term destructured is used to denote the state in which the parameters α_k and ω_k are approaching or are equal to α^*_k and ω^*_k.

The following procedure is developed for the determination of the parameters for the S_BRICK model:

- The geological stress history of the material should be modelled by taking into account the parameters α and ω, which describe the structure. This is necessary for all the kinematic hardening models, since the model response is governed by the initial state and the recent stress-history effects.
- From the drained triaxial tests starting from states $A^\star$ and $C^\star$ (see Figure 4) on the reconstituted material, a maximum angle of shearing resistance, which is here attributed to the critical state angle, is obtained and $\alpha^\star_k$ is determined, yielding the values of φ, as explained by Simpson [27], which are given in the table in Figure 5.
- Parameter $\omega^\star_k$ is always set to zero for reconstituted materials.
- From the drained triaxial tests starting from states A and B the critical state angle for the natural material is obtained and the starting value for α is determined based on the values given in the table in Figure 5.
- From the triaxial tests starting at state C^d the critical state angle is obtained for natural material destructured during compression and a final value α_k is determined based on the values given in the table in Figure 5. If the material has completely lost its structure, α_k is equal to $\alpha^\star_k$.
- Input parameters ω and ω_k are determined with a trial-and-error process so that the measured G_{max} values are reproduced by the model for all three tests starting at states A, B and C. As already indicated, if the material has no structure, ω_k is set to zero.
- From the drained triaxial shearing tests starting at states A and C, the destructurisation parameters for shearing x^{sh}_1, x^{sh}_2, y^{sh}_1 and y^{sh}_2 are determined through a comparison of the model's prediction and measured values in q-ε_a and G-ε_s diagrams using a trial-and-error process. Because the volumetric deformations and hence destructuring due to volumetric deformation in shearing are prevented in undrained stress paths, the parameters y^{sh}_1 and y^{sh}_2 are determined from undrained tests. These values can be used to determine the volume change and are than used in drained tests to obtain the parameters x^{sh}_1 and x^{sh}_2.
- From the results of the isotropic compression on natural material between the state points B and C^d, the destructuration parameters for the compression x^c_1 and x^c_2 can be obtained. Similarly, the parameters for swelling can be obtained for recompression (x^{sw}_1 and x^{sw}_2) between the states B and A.

Using the proposed parameter-determination procedure, a unique set of parameters is obtained for a particular material. As will be shown latter, the stress-strain behaviour was modelled to a high degree of accuracy for Pappadai clay, for which the procedure was strictly followed, and to some degree also for Corinth marl with a similar result. However, not all the materials are usually studied in such detail and many of the required tests might not be available. It is demonstrated later, on the example of North-Sea clay that a satisfactory result can also be obtained in such a case.

To summarise, the full implementation of structure and destructuring as implemented here requires the determination of the additional sixteen parameters in total. As will be demonstrated later, this number can be significantly reduced due to the robustness of the model. Four of them (α, α_k, ω and ω_k) represent the structure and twelve $(x_i, y_i)^{c,sh,sw}$ represent the rate of destructurisation in compression, swelling and shearing. A volumetric component of destructuring is present in all the drained stress paths, while shear components are present in all but the isotropic compression and swelling stress paths. It is still not clear whether or not the shear components of the plastic strains have a noticeable influence on stress paths with no significant change in the deviator component, for example, in the normal compression and the recompression stress paths. Amorosi and Kavvadas [1] argue that for those stress paths only isotropic hardening and destructuring due to volumetric plastic strain have a noticeable effect. If this is the case, then the number of necessary parameters could be reduced to twelve. It is reasonable to expect that not all the types of destructuring are present for a dominant stress path, so the necessary number of total additional parameters for destructuring can be as low as four. The modelling of destructuring is implemented in such a way that the model parameters that are not significant can be omitted without hindering the model's behaviour.

4 PRESENTATION OF THE S_BRICK MODEL ON A CONCEPTUAL LEVEL

The capabilities of the S_BRICK model to simulate the structure and destructuring are presented by comparing the numerical results of the two conceptual materials taken at the different stress-strain paths for the two different states. Both materials have all the basic parameters equal, and they are the same as parameters given for London clay [27], which are summarised in Table 1, except for the amount of structure modelled. Material B represents the material with the stronger structure (α^B=1.1 and ω^B=0.5) and material A represents the material with the weaker structure (α^A=0.7 and ω^A=0.0). Using the structure parameters given for material A, the S_BRICK model is basically reduced to being the same as the basic BRICK model for London clay [27].

4.1 Results of the modelling of structure on a conceptual level using S_BRICK

The influence of the structure parameters α and ω on the increase in strength, stiffness and the SBS is presented by comparing the S_BRICK predictions for materials A and B. The purpose of showing the comparison is to demonstrate that S_BRICK is capable of modelling the main features of the theoretical framework for structural soils proposed by Cotecchia and Chandler [14].

S_BRICK predictions for stress paths that comprise normal compression, swelling, and drained triaxial shearing for materials A and B are shown in the *v-logp'* plane in Figure 6. The predictions of the normal compression lines (NCLs) and the critical state lines (CSLs) for both materials are also shown in the figure. The numerical triaxial tests were taken at different states (OCR varies from 1 to 10). It is evident that the CSL^B and NCL^B lie to the right of the CSL^A and NCLA, as is expected for the material of stronger structure. It is clear that the distance between the CSL^B and NCL^B is greater than the distance between CSL^A and NCL^A, which is also expected for a material of stronger structure. Furthermore, it can be observed that S_BRICK made a prediction, which can be interpreted for each material as an almost unique position of CSL, regardless of the state in which the shearing tests were modelled. Therefore, the unity of the position of the CSL line was anticipated in the continuation on a conceptual level to interpret the other data.

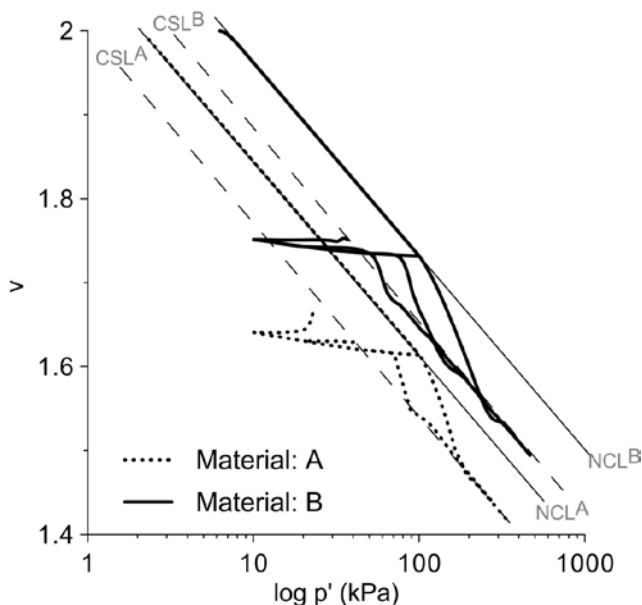The results for different drained shearing stress paths in the *q-p'* space for normally consolidated material (OCR=1) and overconsolidated material (OCR=10) are shown in Figure 7. It was demonstrated that the material with a stronger structure (B) reached higher peak deviatoric stresses than the material with a weaker structure (A), regardless of the direction of the stress path and the state at which they were started. The stress paths in compression produced higher inclinations for the CSL lines than in the extension, which is expected. For the model of the over-consolidated test the increase of the peak deviatoric stress due to the over-consolidation and subsequent softening towards the CSL line is also evident. It was also observed, but not shown here, that the material with the stronger structure (B) has higher stiffness in the range from vary small (i.e., below 0.001%) to large strains (i.e., above 1%) in both compression and extension.

The SBSs predicted by the model for both materials are shown by the dotted lines in Figure 8a, in which the results from the triaxial shearing at different levels of over-consolidation are presented. The results are shown as a normalized plot in the q/p'^A_e - p'/p'^A_e plane, where p'^A_e represents the equivalent pressure taken on a normal compression line of the material A. (The 50% destruc-turisation case shown in the figure will be considered later.) It is evident that the material B has a much larger SBS than the material A, which is expected for a material with a stronger structure. In Figure 8b the results are further normalized with the inclusion of structure (*S*) in the q/Sp'^A_e - p'/Sp'^A_e plane. It can be seen that the normalised SBSs of the materials A and B coincide, as suggested by the theoretical framework for structured materials, given by Cotecchia & Chandler [14].
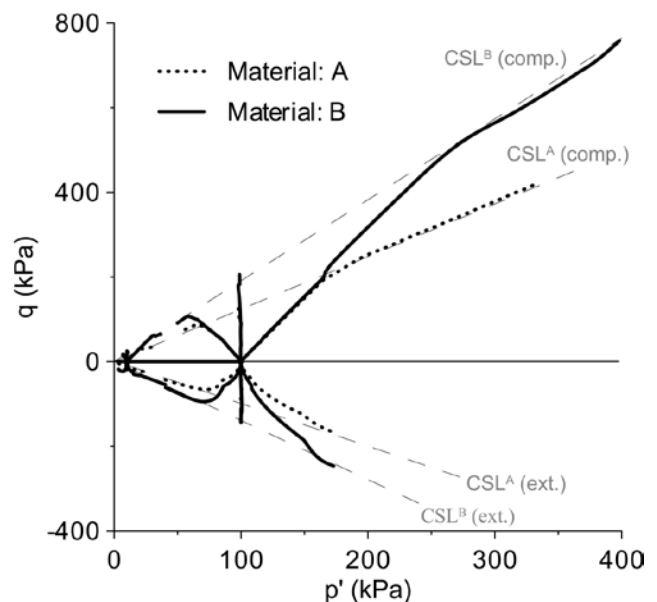

Figure 6. S_BRICK predictions of normal compression and swelling with drained triaxial shearing taken at different states for the materials *A* and *B*.

Figure 7. S_BRICK predictions of drained triaxial shearing taken at different directions for the normally consolidated and overconsolidated state (OCR=10) for the materials *A* and *B*.
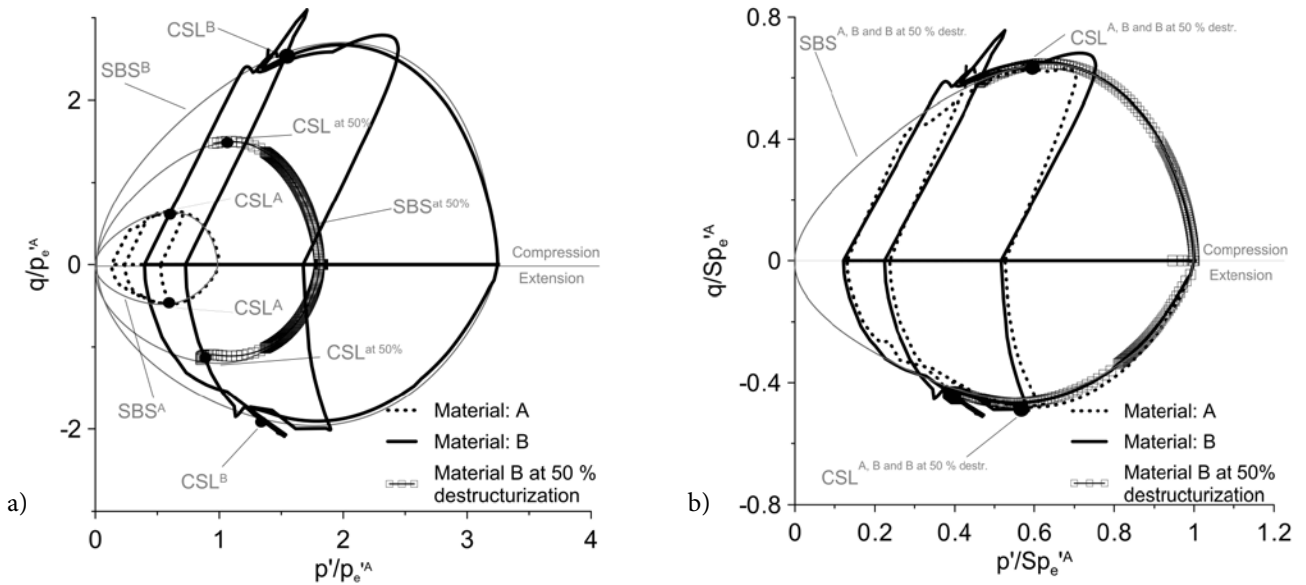
Figure 8. State boundary surfaces predicted by S_BRICK for materials *A*, *B* and material *B* with 50% destructurisation before shearing in: (a) q/p'^A_e - p'/p'^A_e plot and (b) q/Sp'^A_e - p'/Sp'^A_e plot.

4.2 Results of the modelling of destructuring on a conceptual level

The results of destructuring as modelled by S_BRICK in compression, swelling and shearing are shown by comparing the same two conceptual materials A and B. The results of destructuring in compression are shown in Figure 9a, where the parameters α and ω were reduced at different rates to 50 % of the initial values for the

material B (α^B_k=0.9 and ω^B_k=0.25). For demonstration purposes, the parameters x^c_i, y^c_i (i=1,2), describing the rate of destructuring in normal compression, are the same for the volumetric and the deviatoric component. The values that were used are x^c_i, y^c_i=1000 for the fastest rate of destructuring; x^c_i, y^c_i=500 for the intermediate rate and x^c_i, y^c_i=200 for the slowest rate of destructuring. It is evident from Figure 9a that all three tests reach the normal compression line that lies in-between the normal
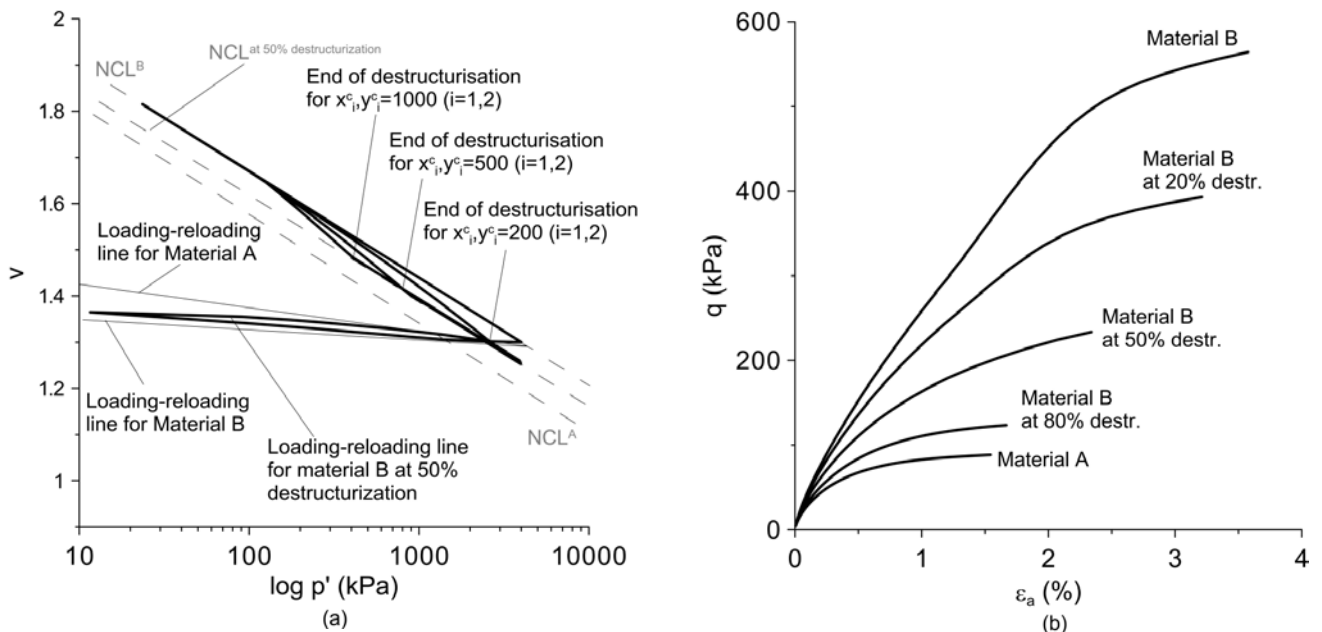

Figure 9. Different rates of destructuring at normal compression and destructuring in swelling modeled with S_BRICK (a) and different levels of destructuring for the triaxial shearing modeled with S_BRICK (b).

compression lines for materials A and B, but at different rates, as expected.

The modelling of destructuring in swelling is also presented in Figure 9a, in which the structure parameters α and ω for the material B were again allowed to reduce to 50 % of the initial values. The swelling line of the destructured material is presented together with the normal compression and swelling lines of the materials A and B. It can be seen that the slope of the swelling line of the destructured material lies in-between the swelling lines of the materials A and B. Furthermore, it can be seen that the material destructured in swelling reaches the same normal compression line after recompression as materials that were destructured in compression. The results of a triaxial shearing test after destructurisation in compression are also shown in Fig 8 in the form of normalised plots. In Figure 8a, the SBS for material B at 50 % destructurisation clearly lies in-between the SBSs for materials A and B, while in Figure 8b they all coincide, as one would expect according to the theoretical framework.

Finally, the modelling of destructuring in shearing is presented in Figure 9b, where the structure parameters for material B have been allowed to reduce for 20, 50 and 80%. A clear trend of reducing the peek deviator value from material B towards material A can be seen with the increasing amount of destructurisation.

5. THE S_BRICK PREDICTION OF STRESS STRAIN BEHAVIOUR OF PAPPADAI CLAY, NORTH SEA CLAY AND CORINTH MARL

The S_BRICK model was validated using the laboratory results from the three different materials, which could be classified as hard soils and soft rocks according to their strength and mechanical behaviour. The Pappadai clay, North Sea clay and Corinth marl were chosen to demonstrate the ability of the S_BRICK model to cover a wide range of structured materials. The key parameters of the S_BRICK model for each natural material are given in Table 1. All the other necessary parameters for the S_BRICK model were taken as constants and were the same as the parameters for the BRICK model of London clay [27]. A list and description of the validated laboratory tests from Pappadai clay, North-Sea clay and Corinth marl are presented in Table 2.

5.1 S_BRICK prediction of the stress strain behaviour of Pappadai clay

Pappadai clay has been extensively studied over the years and its behaviour is well documented [13, 12, 14]. It is a hard over-consolidated clay with a weak cementation. According to Cotecchia and Chandler [13], the geological history of Pappadai clay followed four stages: 1) normal consolidation with the structure formation at the end

Table 2. List and description of validated laboratory tests from Pappadai clay, North-Sea clay and Corinth marl.

Pappadai clay			North Sea clay			Corinth marl		
Test label and type	p' (kPa) prior to shearing	OCR prior to testing	Test label and type	p' (kPa) prior to shearing	OCR prior to testing	Test label and type	p' (kPa) prior to shearing	OCR prior to testing
TN-14-D	500	3.4	TT-1-D	10	31	cd-98-D	98	13.3
TN-15-D	800	2.1	TT-2-D	25	16	cd-294-D	294	4.4
TN-16-D	1300	1.3	TT-3-D	50	8	cd-500-D	500	2.6
TN-17-D	2500	1	TT-4-D	760	1	cd-3000-D	3000	1
TN-18-D	1500	1.1	TT-5-D	10	70	cd-6000-D	6000	1
TN-20-D	250	6.8	TT-6-D	25	28	cd-56-U	56	23.2
TN-5-U	700	2.4	TT-7-D	50	14	cd-315-U	315	4.1
TN-6-U	300	5.7	TT-8-D	700	1	cd-550-U	550	2.4
TN-7-U	500	3.4	TT-9-D	10	86	cd-3000-U	3000	1
TN-10-U	1300	1.3	TT-10-D	25	34	cd-5000-U	5000	1
TN-11-U	1600	1.1	TT-11-D	50	17			
TN-12-U	3800	1	TT-12-D	860	1			
TN-21- K_0		1	TT-2r-D	25	13			
			TT-12r-D	800	1			

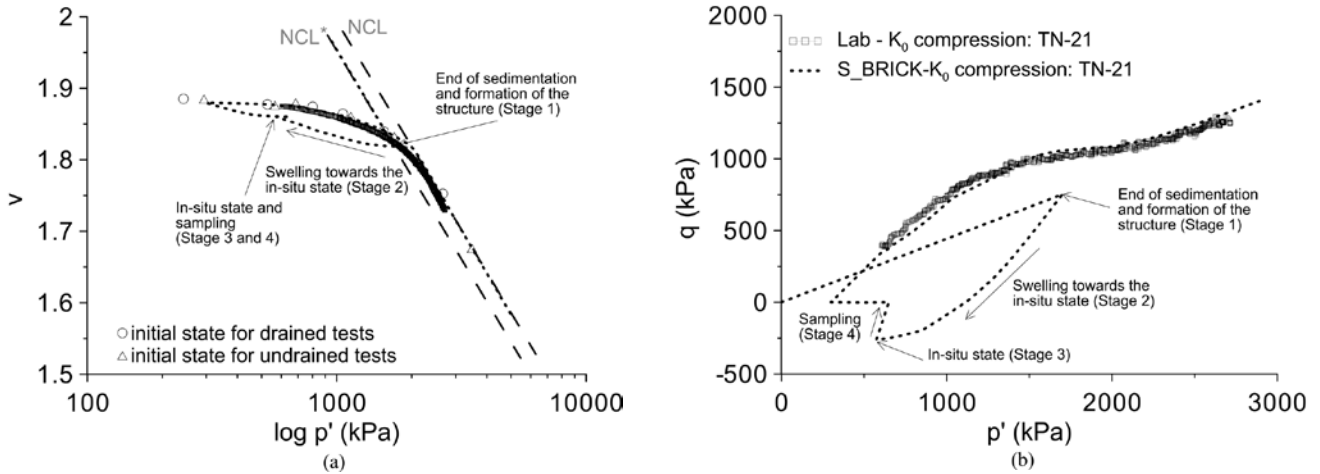D- Drained triaxial shearing   U- Drained triaxial shearing K_0 -Triaxial K_0 compression test

Figure 10. S_BRICK prediction of Pappadai clay history in normal compression in: (a) v-logp' (b) q-p' plots.

of sedimentation, 2) overconsolidation, 3) desiccation, oxidation and weathering and 4) unloading caused by the rise of the water table to the present level. The geological

history of Pappadai clay, modelled by S_BRICK, is shown in Figure 11, along with the Cotecchia and Chandler [13] interpretation in both v-logp' and q-p' planes.
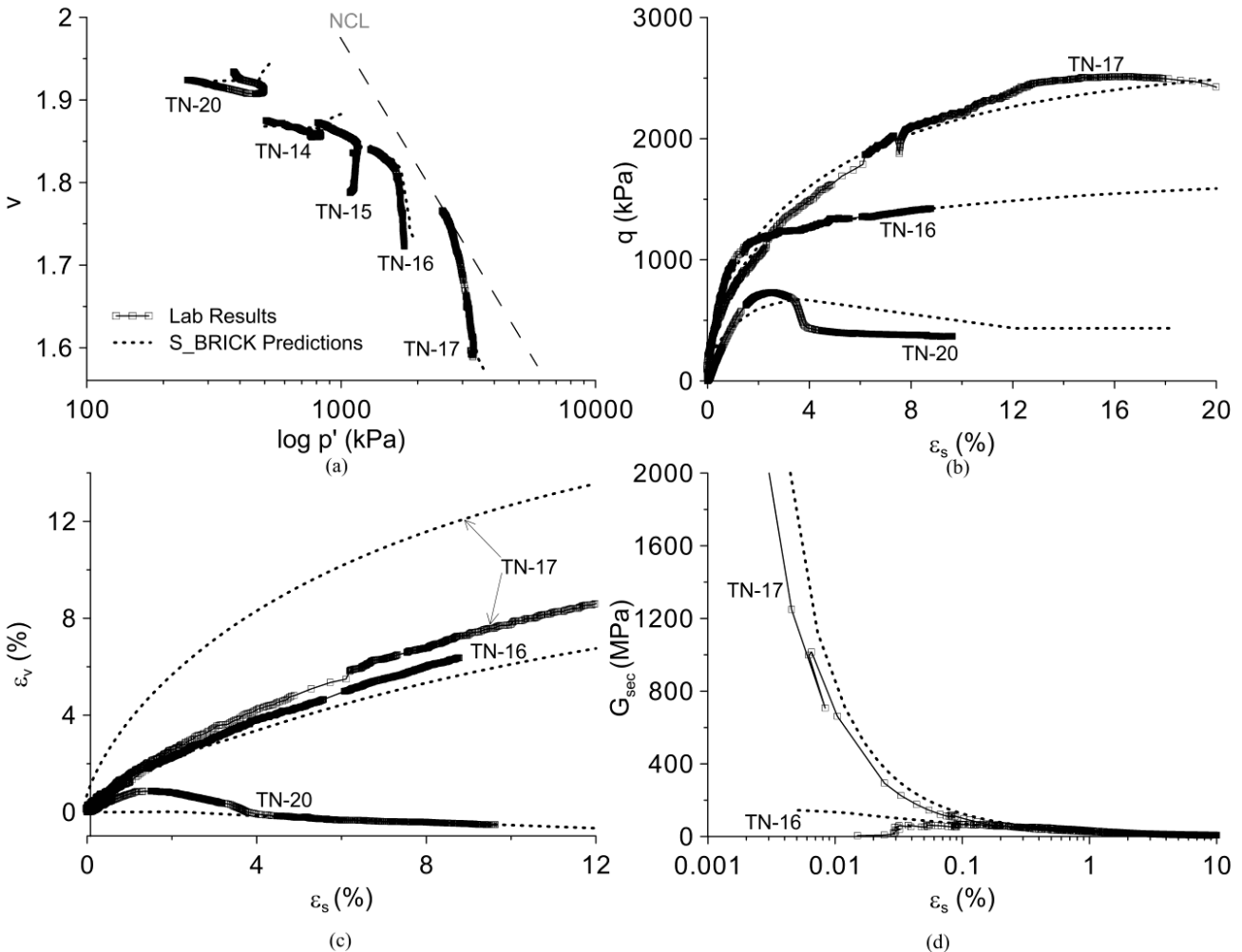

Figure 11. S_BRICK prediction of Pappadai clay behavior for drained triaxial shearing in: (a) v-logp', (b) q-ε_s, (c) ε_v-ε_s and (d) G_{sec}-ε_s plots.

The laboratory tests were carried out by Cotecchia and Chandler [13] on block samples taken from a single depth of 25 m. The material had undrained shear strength measured at around 500 kPa and was over-consolidated with OCR=3. Validation by the S_BRICK model was carried out using six drained and six undrained triaxial shear tests on natural clay (samples TN-6 to TN-20) with the OCR ranging from 1 to 7. The normal compression test was taken on both natural (sample TN-21) and reconstituted clay. The locations of the states of the samples prior to the drained and undrained shearing are shown in Figure 11a.

The key parameters for Pappadai clay, given in Table 1, were derived from the available laboratory data from the natural and reconstituted samples. Parameters λ and κ were derived from the compression tests on natural and reconstituted samples. The basic shape of the normalized S-shape curve, the parameters β_G and β_φ and the parameter ι were taken from the values published for London clay by Simpson [27, 29]. Based on the measured values of G_{max} in Pappadai clay the value of parameter ι was subsequently determined. The parameters for modelling the structure were derived following the previously explained procedure by using the three triaxial drained tests TN-20 (test from state A), TN-18 (test from state B) and TN-17 (test from state C). A critical state angle for the reconstituted ($\varphi_{cs}{}^\star=18°$) and the natural clay ($\varphi_{cs}=21°$), given by Cotecchia and Chandler [14], was taken, leading to the values of $\alpha^\star=0.6$ and $\alpha=0.7$. The values of α_k, ω and ω_k were also determined using the procedure previously explained. The numerical procedure of the modelled strength and stiffness response gave an indication that the destructuring was certainly present in compression, while in recompression and shearing no destructuring was evident, so it was not accounted for. Consequently, only six additional parameters were necessary to take into account the structure and destructurisation of Pappadai clay using the S_BRICK model.

For the S_BRICK model, as for the other kinematic hardening models, it was necessary to model the geological history of the Pappadai clay in order to arrive at the current in-situ state. The sedimentation was modelled with the parameters for the reconstituted clay and at the end of sedimentation phase (formation of structure), the parameters describing the structure were added. Swelling to the in-situ state and sampling was therefore modelled using the parameters for the natural clay. This was the starting point for all the further A-class predictions of the results of laboratory tests, i.e., no changes to any S_BRICK parameters were made from this point onwards.

The S_BRICK predictions of the stress and strain behaviour of the drained triaxial shearing of Pappadai clay are shown in Figure 11. The figure shows separately (a) the compression behaviour in the v-logp' plane, (b) the mobilisation of the deviator stress q with the shear strain ε_s, (c) the variation of the volumetric strain e_v with the shear strain ε_s and (d) the degradation of the secant shear modulus G_{sec} against the logarithmic shear strain ε_s. For clarity, only the three tests TN-20 (OCR=6.8), TN-16 (OCR=1.3) and TN-17 (NC, OCR=1.0) are shown in Figure 11b-d, while the results of the tests of the other samples were qualitatively similar. It can be seen that S_BRICK gave generally excellent predictions of the strength and stiffness behaviour for the entire range of deformations, regardless of the level of overconsolidation. Somewhat less successful were the predictions of the post-peak softening (Figure 11b) and the volumetric behaviour of the sample TN-17 in which the volumetric response was clearly over-predicted. As can be seen from Figure 11a, the sample TN-17 was isotropically consolidated beyond the initial SBS, so a destructurisation in compression was modelled, which could be a reason for the over-prediction of the volumetric response. When a normalization of a p'-q plane is applied, dividing p' and q by $p'^\star_e$, it can be seen in Figure 12a that S_BRICK correctly predicts the position of the stress path for TN-17, which lies in between the SBS for the natural and reconstituted clay, while all the other results also correctly predict the shape of the SBS for the natural Pappadai clay. When further normalization, that includes the structure (S) is applied (Figure 12b), the SBS for the natural, reconstituted and destructured clay coincides for all the S_BRICK predictions as well as for the samples of Pappadai clay.

The undrained shearing tests were also modelled using the same set of parameters given in Table 1 for Pappadai clay. The S_BRICK predictions of the stress and strain behaviour of the undrained triaxial test are shown in Figure 13a-d in the following diagrams: (a) compression behaviour in the v-logp' plane, (b) mobilisation of the deviator stress q with the mean effective stress p', (c) mobilization of the deviator stress q with the shear strain ε_s and (d) degradation of the secant shear modulus G_{sec} against the logarithmic shear strain ε_s. For clarity, only the three tests TN-7 (OCR=3.5), TN-10 (OCR=1.3) and TN-12 (NC, OCR=1.0) are shown, while the results of the tests of the other samples were qualitatively similar. Generally, it can be concluded that the S_BRICK model gave good predictions of the undrained shear strength and stiffness decay with the deformation of the Pappadai clay samples. It was slightly less successful in modelling the post peak behaviour (Figure 13c) and it predicted somewhat different stress paths in the q-p' plane (Figure 13b) for the over-consolidated samples. When the normalization for $p'^\star_e$ (Figure 14a) is applied, it can
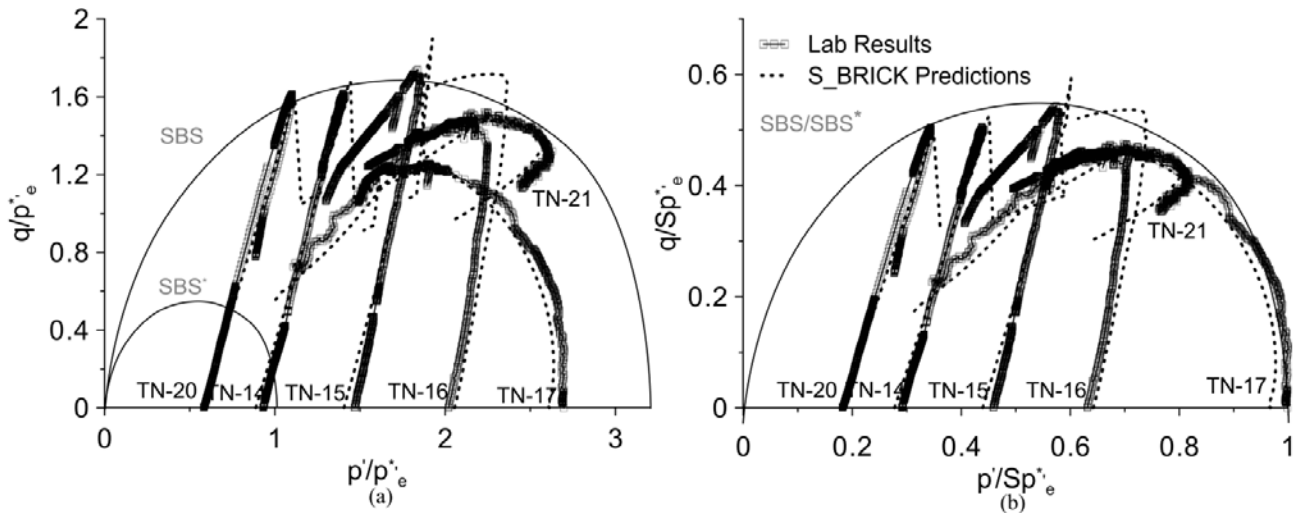
Figure 12. Laboratory and numerical results for drained triaxial tests on Pappadai clay in: (a) q/p'^{*}_e - p'/p'^{*}_e and (b) q/Sp'^{*}_e - p'/Sp'^{*}_e plots.
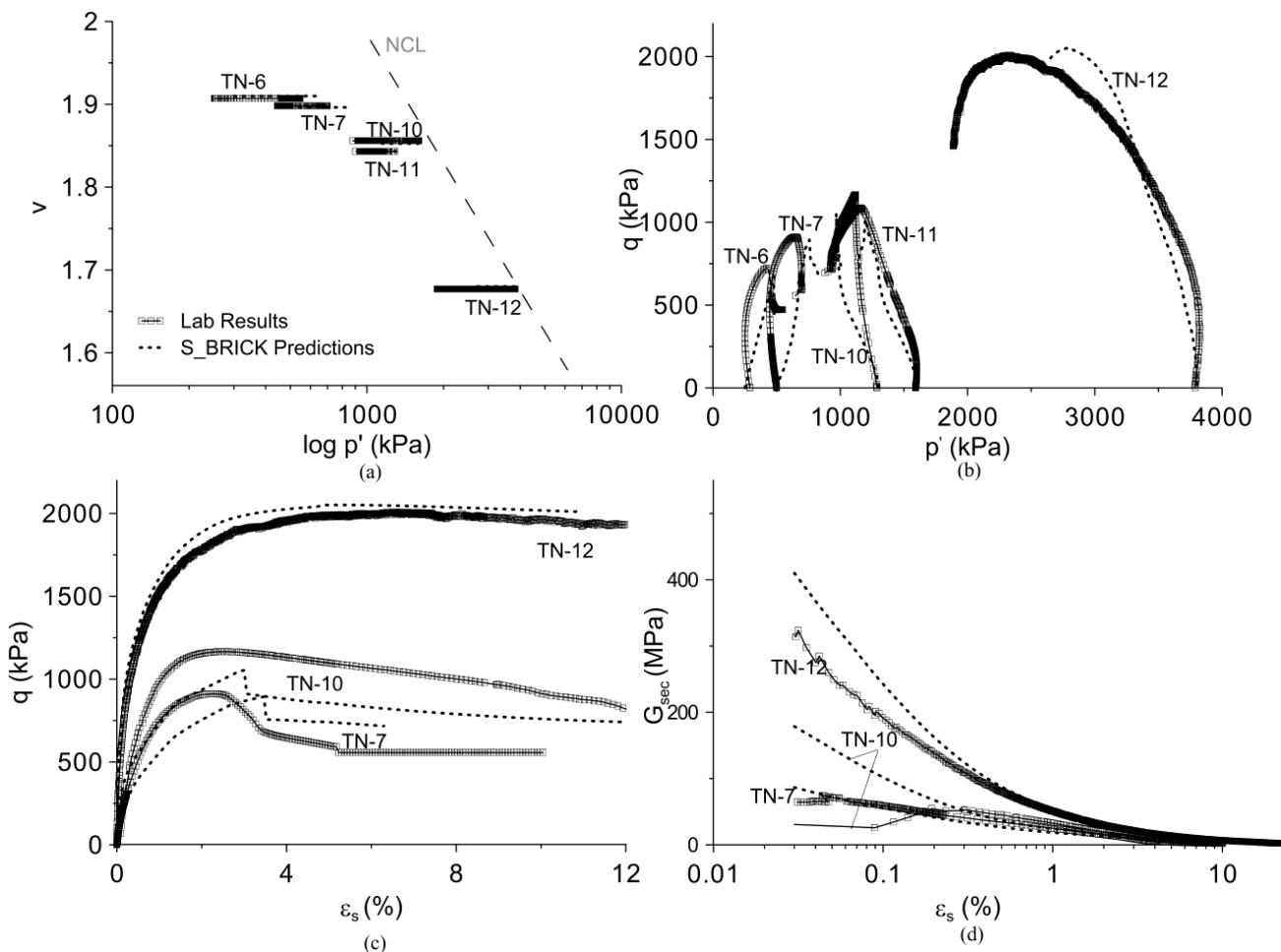

Figure 13. S_BRICK prediction of Pappadai clay behavior for undrained triaxial shearing in: (a) v-logp', (b) q-p', (c) q-ε_s and (d) G_{sec}-ε_s plots.

be seen that the test TN-12 lies inside the SBS for the natural clay, which is attributed to the destructurisation that occurred during compression. Similarly as for the

drained results, when further normalization with the structure parameter S (Figure 14b) is applied, all the results coincide within the boundaries of a single SBS.
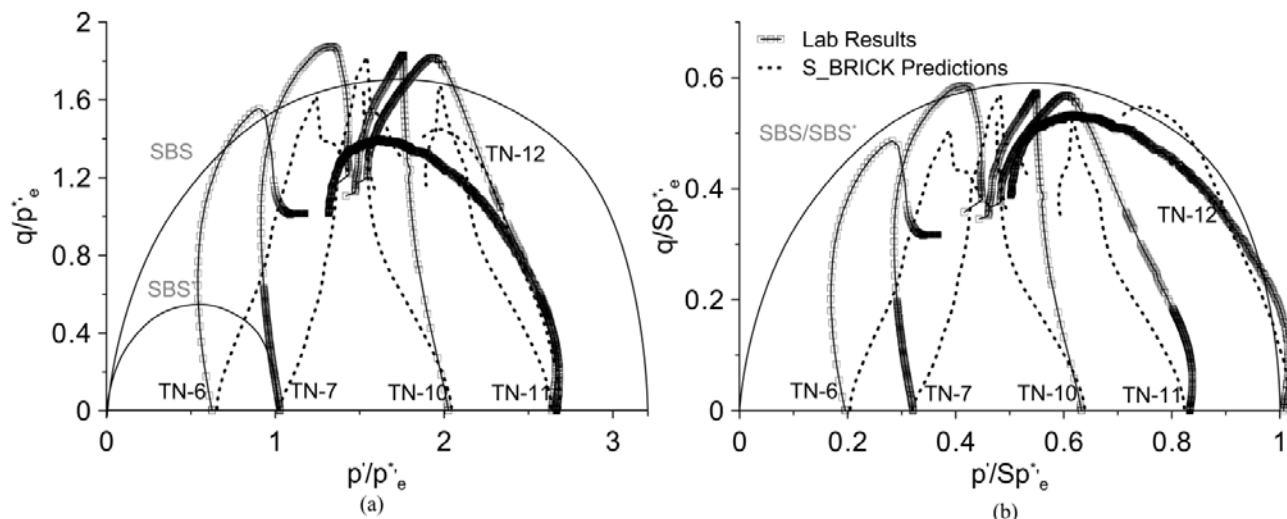
Figure 14. Laboratory and numerical results for undrained triaxial tests on Pappadai clay in: (a) q/p'^{*}_e - p'/p'^{*}_e and (b) q/Sp'^{*}_e - p'/Sp'^{*}_e plots.

5.2   S_BRICK prediction of the stress-strain behaviour of stiff North-Sea clay

The stress-strain behaviour of North-Sea clay was investigated by Jovičić et al. [20]. The investigated clay samples were taken from depths between 15 and 75 m from two different formations: the Cape Shore formation (depths between 15 and 40m) and the Ferder formation (depths between 40 and 75m). According to Johnson et al. [19] the clays from both formations are generally similar, but distinguished mainly by the values of the high undrained shear strengths found at the top of the formations (Figure 15), which is the result of breaks in the depositional sequence. A high calcium content (up to 13%) and a high undrained shear strength strongly suggested that the material is cemented.

Jovičić et al. [20] reported drained triaxial tests investigating the strength and stiffness of two reconstituted (TT-2r and TT-12r) and twelve natural samples (TT-1 to TT-12) of the clay. The tests were carried out at in-situ stresses and also when swelled back to effective stresses as low as 10 kPa. In addition to the laboratory testing, the paper reported class-A predictions (e.g., using a single set of pre-determined parameters) of the behaviour of the North-Sea clay using the basic BRICK model. As a continuation of their work, a set of class-A predictions of those tests were subsequently modelled using the S_BRICK model and compared with the laboratory data and the prediction of the basic BRICK model.

The input parameters for modelling North Sea clay, taken from Jovičić et al. [20], are shown in Table 1. The procedure for the determination of the parameters describing the structure could not be followed in full in this case as the tests were not originally designed for

that purpose. The adopted approach was to model the amount of overconsolidation for each individual sample in accordance with the estimated level of additional overburden (Figure 15) at the depth of the sampling. The
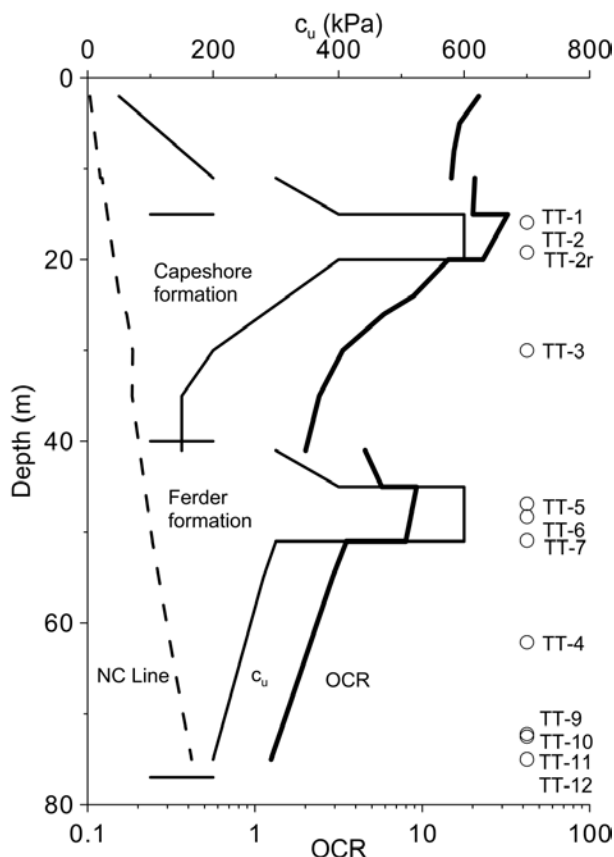

Figure 15. North-Sea clay undrained shear strength profile with sample location and estimated OCR profile (after Jovičić et al. [20]).

difference in the approach taken by Jovičić et al. [20] was that the influence of the structure was accounted for, so that realistic levels of the estimated over-consolidation, based on the measured values of undrained shear strength, could have been used.

The parameters $\alpha^\star$ and $\omega^\star$ were determined from the critical state angle of the shearing resistance for the reconstituted clay, which were obtained from the two triaxial shearing tests on reconstituted samples. Based on the available results, the parameter α was taken to be the same as for the reconstituted material and the parameter ω was determined by taking into account the small strain stiffness response of the clay. The parameter ω_k was determined by matching the strength and stiffness at the critical state after the destructurisation was finished. Since no study of the influence of compression and swelling on the destructurisation was carried out for the North Sea clay, it was first estimated that only a destructurisation in shearing is present. However, even with the structure and the destructurisation in shearing taken into account, it was still not possible to satisfactorily reproduce the stress-strain response of the soil. It was concluded that the North-Sea clay has probably a structure that is sensitive to both swelling and compression, to which the samples were exposed during sampling and subsequent shearing stress paths. This was particularly relevant for the samples that were swelled to low confining pressures. The parameters for describing the destructurisation both in swelling and compression were determined through a trial-and-error process. For the samples taken from the Cape Shore and Ferder formations different parameters describing the structure and destructurisation were obtained, as can be seen from Table 1, with the Cape Shore formation featuring a stronger structure.

Most of the shear tests in the original laboratory programme were taken after the swelling to a low effective stress. From the Cape Shore formation, four samples were modelled: TT-1 (sheared from p'=8 kPa, OCR=31), TT-2 (sheared from p'=25 kPa, OCR=16), TT-3 (sheared from p'=50 kPa, OCR=8) and reconstituted clay TT-2r (sheared from p'=25 kPa, OCR=12). From the Ferder formation nine samples were modelled, but for clarity only the results from the four samples are shown: TT-12 (sheared from p'=800 kPa, NC), TT-8 (sheared from p'=650 kPa, NC), TT-11 (sheared from p'=200 kPa, OCR=3.2), and TT-6 (sheared from p'=25 kPa, OCR=28). The S_BRICK prediction of the triaxial shearing tests of the samples from the Cape Shore and Ferder formations are shown in Figure 16 and Figure 17, respectively. Each figure shows separately (a) the variation of the deviator stress q and the axial strain ε_a, (b) the variation of the volumetric strain ε_v with the
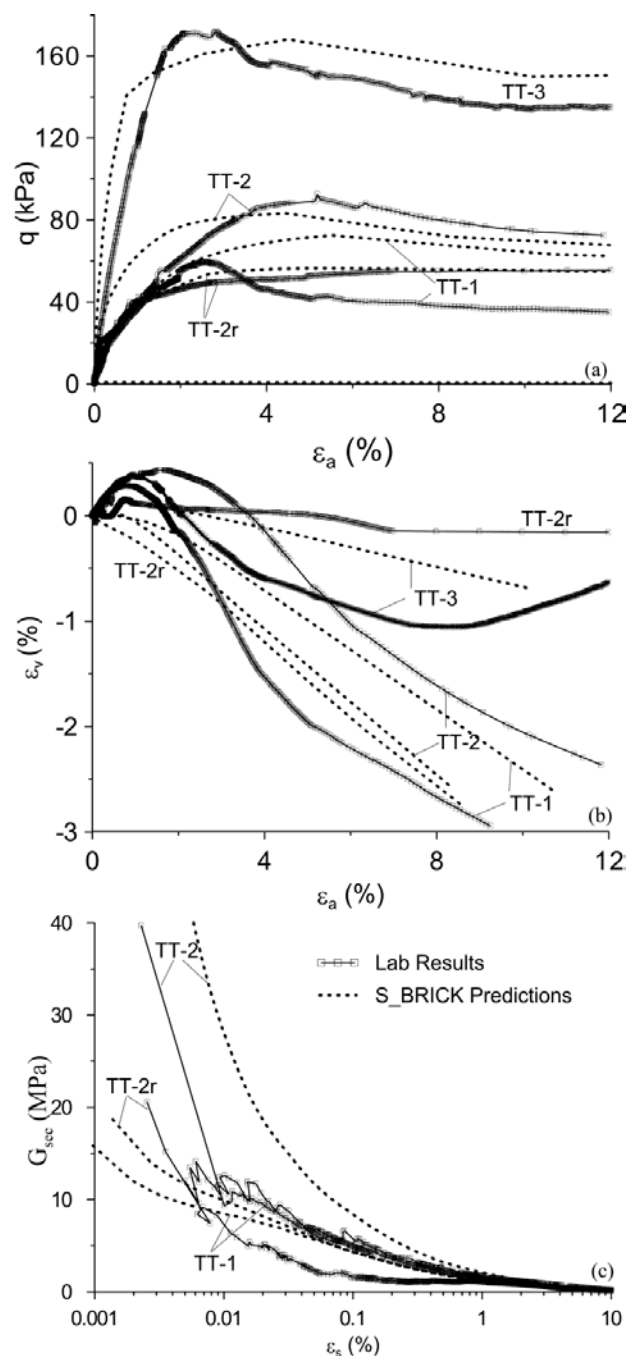

Figure 16. S_BRICK prediction of North-Sea clay behavior for drained triaxial shearing (Cape Shore formation – depth 15-30m) in: (a) q-ε_a, (b) ε_v-ε_a and (c) G_{sec}-ε_s plots.

axial strain ε_a and (c) the degradation of the secant shear modulus G_{sec} against the logarithmic shear strain ε_s.

It can be seen from the figures that the S_BRICK model has reasonably well reproduced behaviour for the samples of both clays, and also for the reconstituted material. The peak deviator stresses shown in Figure 16a and Figure 17a were correctly predicted; however,
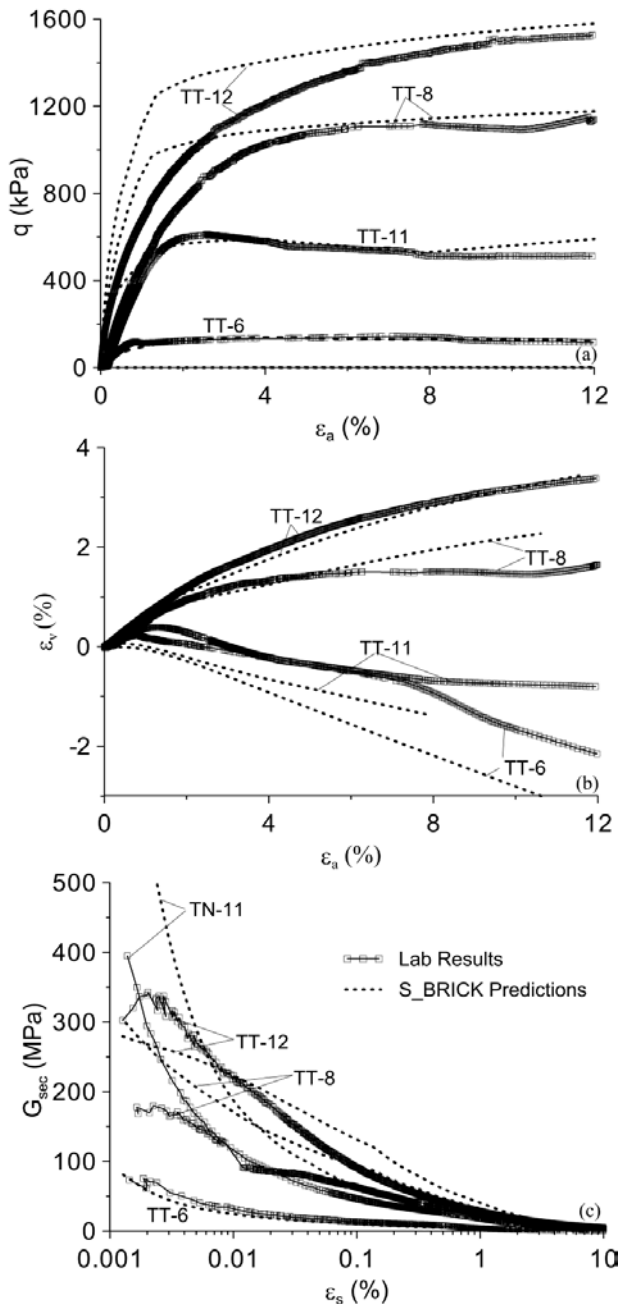
Figure 17. S_BRICK prediction of North-Sea clay behavior for drained triaxial shearing (Ferder formation– depth 45-75m) in: (a) q-ε_a, (b) ε_v-ε_a and (c) G_{sec}-ε_s plots.
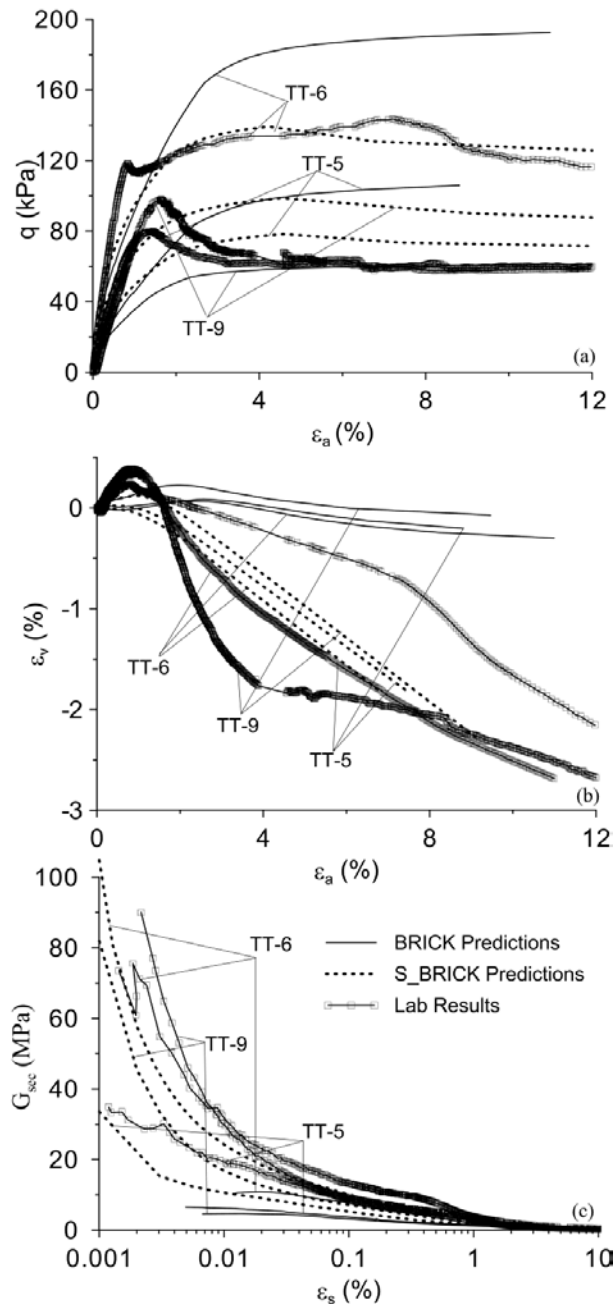
Figure 18. Comparison between S_BRICK and BRICK predictions of North-Sea clay behavior for drained triaxial shearing in: (a) q-ε_a, (b) ε_v-ε_a and (c) G_{sec}-ε_s plots (BRICK predictions after Jovičić et al. [20]).

the model gave a somewhat stiffer response, which can be clearly seen in Figures 16c and 17c, in which the shear stiffness degradation is shown. The volumetric behaviour shown in Figure 16b and Figure 17b, has been generally well predicted, with the model correctly predicting dilation or contraction. When comparing the results published by Jovičić et al. [20] on the same set of laboratory data using the basic BRICK model without

structure, a significant improvement can be observed using S_BRICK, as it can be seen in Figure 18. The S_BRICK prediction of the peak deviator strength falls within the range ±15%, when comparing to the laboratory results, while the BRICK prediction falls well below that (Figure 18a). Also, a significantly better prediction was obtained when comparing the shear moduli at different strain magnitudes, ranging from 0.001% to 1%

(Figure 18c). The motivation for the development of the S_BRICK model was to improve the predictions of the BRICK model for the behaviour of North Sea clay. These results clearly demonstrate the necessity for the structure to be accounted for in the constitutive modelling of this natural material [31, 32].

5.3 S_BRICK prediction of the stress-strain behaviour of Corinth marl

The S_BRICK prediction of the stress-strain behaviour of Corinth marl was based on the published data from the literature [3,9,10]. According to the different authors, Corinth marl is heavily cemented, predominantly carbonate material (up to 75 % of the carbonate content), for which the cementation occurred at the end of the sedimentation. The investigated Corinth marl was taken from a depth of 60m, at the base of the Corinth canal. The samples had a measured high, undrained shear strength (c_u=2000 kPa), and were overconsolidated (OCR=2.5) in the in-situ state. The S_BRICK model was validated using the laboratory results from the five drained and the five undrained triaxial shear tests, with the OCR varying between 1 and 24 and on one normal compression test.

The parameters λ and κ given in Table 1 were taken from Burland et al. [10]. The previously explained procedure was followed to determine the parameters ω and ω_k. The procedure was based on the three triaxial drained tests cd98 (test from state A), cd3000 (test from state B) and cd6000 (test from the state C). The critical state angle of the shearing resistance of 33.4° given by Anagnostopoulos et al. [3] was used, yielding a value for α=1.1. The analysis of the available data showed that the destructuring was present both in compression and in shearing. The influence of the deviatoric component was

determined from the undrained tests, and the influence of the volumetric component from the drained tests.

As with the Pappadai clay, the stress history was modelled comprising sedimentation, formation of the structure, overconsolidation to the in-situ state and subsequent sampling and consolidation. The results of the S_BRICK prediction are shown in Figure 19: a) in the v-logp' plane and b) in the q-p' plane. It can be seen that the S_BRICK model correctly predicted both the normal compression line for the reconstituted (NCL*) and natural (NCL) Corinth marl. It also correctly predicted the compression and the recompression behaviour as well as the yielding pressure in compression, given by Bressani [9].

The Class-A predictions of the S_BRICK model are shown in Figure 20, along with the results of the drained tests on the three samples: cd98 (sheared from p'=98 kPa, OCR=13.3), cd294 (sheared from p'=294 kPa, OCR=4.4) and cd500 (sheared from p'=500 kPa, OCR=2.6). The figure shows: (a) the variation of the deviator stress q with the axial strain ε_a, (b) the variation of the volumetric strain ev with axial strain ε_a and (c) the degradation of secant shear modulus G_{sec} against the logarithmic axial strain ε_a. It can be observed that the S_BRICK model has correctly predicted the peak deviator stress (Figure 20a) and the mobilisation of the stiffness with the shear strain (Figure 20c). The stiffness degradation prediction was good, but the comparison is hampered by the limitation of the available laboratory data with the stiffness measured only up to 0.1%. The prediction of the volumetric behaviour shown in Figure 20b was generally good, with the model correctly predicting the dilative or contracting behaviour. The results from the prediction of the undrained shearing are shown in Figure 21 in the form of a q-p' plot. The five tests
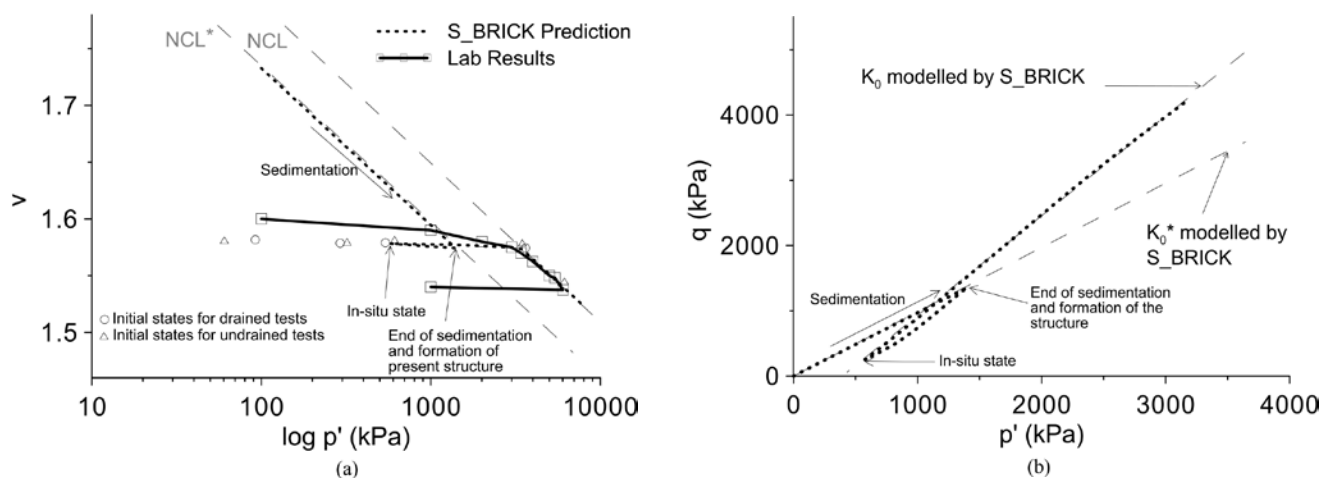

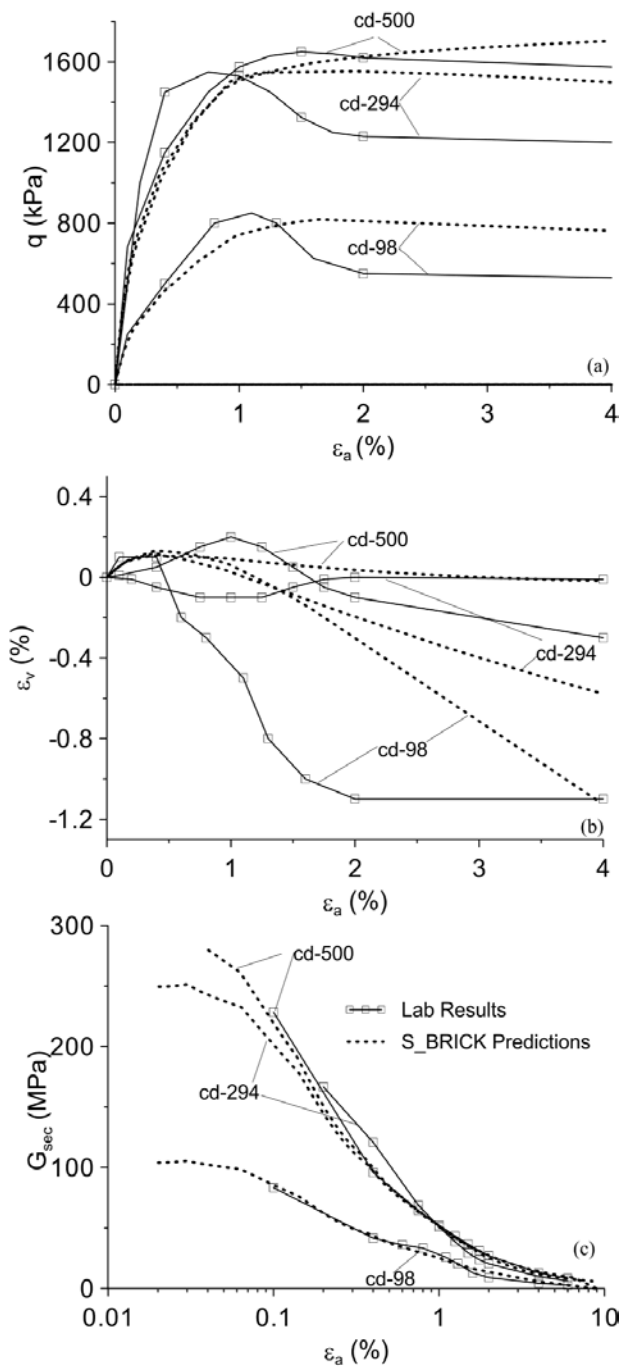**Figure 19**. S_BRICK prediction of Corinth marl history in normal compression (a) v-logp' (b) q-p' plots.

Figure 20. S_BRICK prediction of Corinth marl behavior for drained triaxial shearing in: (a) q-ε_a, (b) ε_v-ε_a and (c) G_{sec}-ε_s plots.

Figure 21. S_BRICK prediction of Corinth marl behavior for undrained triaxial shearing in q-p' plot.

5.4   Discussion

The analysis of the prediction using the S_BRICK model demonstrated that the model was able to predict correctly the main features of the stress-strain behaviour of the three completely different, natural, structured materials. For Pappadai clay and Corinth marl the excellent predictions of the compression behaviour in the v-logp' plane were obtained, with the S_BRICK model essentially correctly predicting the normal compression lines for both the reconstituted and natural material. The condition for this was the correct estimates of the geological histories of the two materials, which were in this case available from the work of the other authors. For all the materials the best results were obtained when predicting the peak strengths in the drained triaxial tests, with an average deviation of less than 5 % and a maximum deviation of no more than 15 %, which was derived only for the very heavily over-consolidated samples of North-Sea clay (TT-1 and TT-10). The undrained shear strengths were also successfully predicted, with an average deviation of under 10%. The analysis of the shear modulus degradation with the strain at a very small strain level (i.e., below 0.001%) was possible only for the North-Sea clay, due to the lack of the laboratory results for the other materials in the range of the small strains. More than half of the predicted shear moduli for all the twelve samples taken at the different strain magnitudes, ranging from very small strains of 0.001% to large strains at 1%, fall within the range of ±25 % difference from the measured values in the laboratory. For both the Papaddai clay and the Corinth marl the prediction was satisfactory for the small (i.e., between 0.01% and 0.1%) but better for the middle strain range (i.e., between 0.1% and 1%) and also at large strains at 1% and above. It is therefore conclusive that the modelling of the shear modulus degradation with the strain at

were carried out on samples taken from the heavily over--consolidated states (sheared from p'=56 kPa, OCR=23) up to the samples consolidated well beyond the yielding pressure (sheared from p'=5000 kPa) in compression. It can be seen that S_BRICK correctly predicted the undrained shear strength and also the undrained shear--stress paths for both the overconsolidated and normally consolidated samples for the full range of stresses.
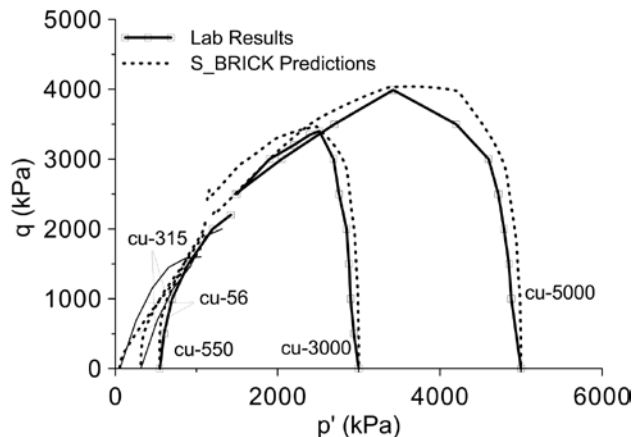
the middle-to-large strain level was generally accurate for all the three materials.

The least successful aspect of the S_BRICK predictions was the volumetric strains. In general, the drained peak strength values were predicted at strains that were somewhat larger than those measured in the laboratory. The model correctly predicts the dilative or contractive response, but the amount of contraction or dilation is not always accurately predicted. In undrained shearing this is also reflected in the prediction of the undrained stress paths. However, the volumetric component of the deformation is a complex phenomenon and the modelling of the volumetric deformation requires more research and a better understanding of the volumetric behaviour in compression, swelling, reloading and shearing.

6   CONCLUSIONS

A model for structured soils named S_BRICK was developed from the basic BRICK model originally published by Simpson [27, 29]. The capabilities of S_BRICK to model the structure and the destructurisation were first demonstrated on a conceptual level within the boundaries of the theoretical framework for structured soils developed by Cotecchia and Chandler [14]. It was shown that the S_BRICK model, extrapolating the concept of the state parameter originally set in the BRICK model, can describe all the main features of the framework for the behaviour of the structured soils. The model also includes the behaviour of the reconstituted materials, as it contains unchanged elements from the original BRICK model.

The S_BRICK model was validated on three natural materials, i.e., Pappadai clay, North-Sea clay and Corinth marl, featuring different origins, geological history, mineralogy, type of structure and over-consolidation. It was shown that S_BRICK was able to successfully capture the stress-strain behaviour typical for those natural structured materials. It can be concluded that S_BRICK, which in itself contains the complete BRICK model, has a universal potential to model a wide range of natural clay soils, including normally consolidated and over-consolidated clays, as well as hard soils and soft rocks.

In its widest form the new model requires a total of 16 additional parameters to describe the structure and destructuring. However, it was demonstrated that for the successful validation of the behaviour of natural materials, only six to seven additional parameters were necessary. In the case of Pappadai clay, which was the most researched material in terms of the origin of structure and destructuring, the predictions were the most accurate and in the best agreement with the theoretical framework for the structured materials. The validation of the North-Sea clay behaviour has also shown that the model is sufficiently robust, even though the geological history is not fully understood, to predict satisfactorily the behaviour of two different formations and without all the necessary tests for the parameter determination. The validation of the behaviour of Corinth marl was more successful, as the origin of the structure and over-consolidation were better understood than that of the North Sea clay.

Additional work on the model still has to be done with regards to the prediction of the volumetric behaviour and the destructuring. The mechanisms of destructuring and the development of the volumetric strains are both clearly affected by the type of plastic strains and are likely to be different in compression, swelling, reloading and shearing. This subject clearly requires more fundamental research on the theoretical and practical levels in the laboratory. The results of the research demonstrate that different causes of the development of volumetric strains were the aspects of the validation that proved to be the most difficult to achieve using the S_BRICK model.

REFERENCES

[1]   Amorosi, A., Kavvadas, M.A. 2002. Critical review of the State Boundary Surface concept in light of advanced constitutive modelling. In Numerical Models in Geomechanics: Proceedings of the 8th International Symposium, NUMOG VIII, Rome, 10–12 April 2002. Edited by G.N. Pande and S.

Pietruszczak. A.A.Balkema, Rotterdam, The Netherlands. pp. 85–90.

[2] Amorosi, A., Rampello, S. 2007. An experimental investigation into the mechanical behaviour of a structured stiff clay. Géotechnique 57, 2, 153-166. https://doi.org/10.1680/geot.2007.57.2.153

[3] Anagnostopoulos, A.G., Kalteziotis, N., Tsiamboas, G.K., Kavvadas, M. 1991. Geotechnical properties of the Corinth canal marls. Geotechnical and Geological Engineering 9, 1, 1-26. https://doi.org/10.1007/BF00880981

[4] Atkinson, J.H., Bransby, P.L. 1978. The Mechanics of Soils: An introduction to Critical State Soil Mechanics. McGraw-Hill.

[5] Atkinson, J.H., Richardson, D., Stallebrass, S.E. 1990. Effect of recent stress history on the stiffness of overconsolidated soil. Géotechnique 40, 4, 531-540. https://doi.org/10.1680/geot.1990.40.4.531

[6] Baudet, B.A. 2001. Modelling effects of structure in soft natural clays. PhD thesis. City University, London.

[7] Baudet, B.A., Stallebrass, S.E. 2004. A constitutive model for structured clays. Géotechnique 54, 4, 269-278. https://doi.org/10.1680/geot.2004.54.4.269

[8] Been, K., Jeffries, M.G. 1985. A state parameter for sands. Géotechnique 35, 1, 99-112. https://doi.org/10.1680/geot.1985.35.2.99

[9] Bressani, L.A. 1993. The secant stiffness behaviour of Corinth Marl. Geotechnical Engineering of Hard Soils and Soft Rocks, Athens Greece, Ed. Anagnostopoulus, A. G. et al., Rotterdam, Balkema, 391-396.

[10] Burland, J.B., Rampello, S., Georgiannou, V.N., Calabresi, G. 1996. A laboratory study of the strength of four stiff clays. Géotechnique 46, 3, 491-514. https://doi.org/10.1680/geot.1996.46.3.491

[11] Clayton, C.R.I., Priest, J.A., Rees, E.V.L. 2010. The effect of hydrate cement on the stiffness of some sands. Géotechnique 60, 6, 435-445. https://doi.org/10.1680/geot.2010.60.6.435

[12] Cotecchia, F. 1996. The effects of structure on the properties of an Italian Pleistocene clay. PhD Thesis, Imperial College, London.

[13] Cotecchia, F., Chandler, R.J. 1995. Geotechnical properties of the Pleistocene clays of the Pappadai Valley, Taranto, Italy. Quarterly Journal of Engineering Geology 28, 5-22. https://doi.org/10.1144/GSL.QJEGH.1995.028.P1.02

[14] Cotecchia, F., Chandler, R.J. 2000. A general framework for the mechanical behaviour of a clays. Géotechnique 50, 4, 431-447. https://doi.

org/10.1680/geot.2000.50.4.431

[15] Ellison, K.C., Kenichi, S., Simpson B. 2012. A strain space soil model with evolving stiffness anisotropy. Géotechnique 62, 7, 627-641. https://doi.org/10.1680/geot.10.P.095

[16] Ferreira, P.M.V., Bica, A.V.D. 2006. Problems in identifying the effects of structure and critical state in a soil with transitional behaviour. Géotechnique 56, 7, 445-454. https://doi.org/10.1680/geot.2006.56.7.445

[17] Gasparre, A., Nishimura, S., Minh, N.A, Coop, M.R., Jardine, R.J. 2007. The influence of structure on the behaviour of London clay. Géotechnique 57, 1, 19-31. https://doi.org/10.1680/geot.2007.57.1.19

[18] Gens, A., Nova, R. 1993. Conceptual bases for a constitutive model for bonded soils and weak rocks. Geotechnical Engineering of Hard Soils-Soft Rocks, Athens, Greece, eds. Anagnostopoulos, A.G. et al., Rotterdam: Balkema, 485-494.

[19] Johnson, H., Richards, P.C., Long, D., Graham, C.G. 1993. The geology of the Northern North Sea. British Geological survey, United Kingdom Offshore Regional Report. HMSO, London.

[20] Jovičić, V., Coop M., Simpson, B. 2006. Interpretation and modelling of deformation characteristics of a stiff North Sea clay. Can. geotech. j. 43, 4, 341-354. https://doi.org/10.1139/t06-007

[21] Kavvadas, M. 2000. General report: Modelling the soil behaviour – Selection of soil parametres. The Geotechnics of Hard Soils-Soft Rocks. (Ed. Evangelista & Picarelli), Balkema, 1441-1481.

[22] Kavvadas, M., Anagnostopoulos, A.G. 1998. A framework for mechanical behaviour of structured soils. The Geotechnics of Hard Soils – Soft Rocks, Ed. Evangelista, A., et al., Rotterdam: Balkema, 591-601.

[23] Kavvadas, M., Amorosi, A. 2000. A constitutive model for structured soils. Géotechnique 50, 3, 263-273. https://doi.org/10.1680/geot.2000.50.3.263

[24] Lambe, T.W., Whitman, R.V. 1969. Soil Mechanics. New York: John Wiley & Sons Inc.

[25] Leroueil, S., Vaugan, P.R. 1990. The general and congruent effects of structure in natural soils and weak rocks. Géotechnique 40, 3, 467–488. https://doi.org/10.1680/geot.1990.40.3.467

[26] Rouainia, M., Wood, M.D. 2000. A kinematic hardening model for natural clays with loss of structure. Géotechnique 50, 2, 153-164. https://doi.org/10.1680/geot.2000.50.2.153

[27] Simpson, B. 1992. Retaining Structures: displacement and design. 32nd Rankine Lecture: Géotechnique 42, 4, 541-576. https://doi.org/10.1680/geot.1992.42.4.541

[28] Simpson, B. 2001. Engineering needs. Proc. 2nd Int. Symp. on Pre-failure Deformation Characteristics of Geomaterials, Torino, volume 2, 1011-1026 (Eds M. Jamiolkowski, R. Lancellotta, D.Lo Presti), Lisse, Swets & Zeitlinger. .

[29] Simpson, B. 2001. BRICK 17, GEO suite for windows. Published on: http://www.oasys-soft-ware.com/product/downloads/geo/brick_Nov01.pdf

[30] Schofield, A.N., Wroth, C.P. 1968. Critical State Soil Mechanics. Maidenhead: McGraww–Hill.

[31] Vukadin, V. 2004. Development of the constitutive model for Soft Rocks and Hard Soils, PhD thesis, University of Ljubljana, Ljubljana.

[32] Vukadin, V. 2007. Modelling of the stress-strain behaviour in Hard Soils and Soft Rocks, Acta Geotechnica Slovenica 4, 2, 4-15.